Book Chapter

Determination of the Heterogeneity of Intramuscular Fat and Visceral Adipose Tissue from Dezhou Donkey by Lipidomics and Transcriptomics Profiling

Mengmeng Li, Mingxia Zhu, Wenqiong Chai, Yonghui Wang, Yinghua Song, Baoxiu Liu, Changyun Cai, Yingzi Song, Xue Sun, Peng Xue and Changfa Wang*

Liaocheng Research Institute of Donkey High-Efficiency Breeding and Ecological Feeding, College of Agronomy, Liaocheng University, China

***Corresponding Author:** Changfa Wang, Liaocheng Research Institute of Donkey High-Efficiency Breeding and Ecological Feeding, College of Agronomy, Liaocheng University, Liaocheng, 252000, China

Published **December 27, 2021**

This Book Chapter is a republication of an article published by Changfa Wang, et al. at Frontiers in Nutrition in September 2021. (Li M, Zhu M, Chai W, Wang Y, Song Y, Liu B, Cai C, Song Y, Sun X, Xue P and Wang C (2021) Determination of the Heterogeneity of Intramuscular Fat and Visceral Adipose Tissue From Dezhou Donkey by Lipidomics and Transcriptomics Profiling. Front. Nutr. 8:746684. doi: 10.3389/fnut.2021.746684)

How to cite this book chapter: Mengmeng Li, Mingxia Zhu, Wenqiong Chai, Yonghui Wang, Yinghua Song, Baoxiu Liu, Changyun Cai, Yingzi Song, Xue Sun, Peng Xue, Changfa Wang. Determination of the Heterogeneity of Intramuscular Fat and Visceral Adipose Tissue From Dezhou Donkey by Lipidomics and Transcriptomics Profiling. In: Eloy A Zepeda-Carrillo, editor. Prime Archives in Nutrition. Hyderabad, India: Vide Leaf. 2021.

Ethics Approval: All experimental procedures involving donkeys were approved by the Liaocheng University Animal Care and Use Committee.

Data and Model Availability Statement: Sequencing data can be found in the Sequence Read Archive at the National Center for Biotechnology Information (BioProject ID: PRJNA751405).

Author Contributions: Mengmeng Li: Conceptualization, methodology, formal analysis, investigation, and writing (original draft and editing). Mingxia Zhu and Wenqiong Chai: Investigation, formal analysis, writing (review and editing), and validation. Yonghui Wang: Software andformal analysis. Yinghua Song, Baoxiu Liu, and ChangyunCai: Investigation andformal analysis. Yingzi Song, Xue Sun, and PengXue: Investigation andresources. Changfa Wang: Supervision, writing (review andediting), and funding acquisition.

Declaration of Interest: All authors have declared no competing financial interests.

Acknowledgements: This work was supported by the Open Project of Liaocheng Universtiy Animal Husbandry Discipline (319312101-10), the Open Project of Shandong Collaborative Innovation Center for Donkey Industry Technology (3193308), the Scientific Research Fund of Liaocheng University (318052019), the Innovation and Entrepreneurship Training Program for College Students (202110447017 and CXCY2021002), the Well-bred Program of Shandong Province (2017LZGC020),the Shandong Province Modern Agricultural Technology System Donkey Industrial Innovation Team (SDAIT-27), and the Taishan Leading Industry Talents-Agricultural Science of Shandong Province (LJNY201713).

Abstract

Intramuscular fat (IMF) and visceral adipose tissue (VAT) are both lipids, but have significantly different deposition processes. Furthermore, the heterogeneity of lipid molecular characteristics and mechanisms is unclear. Accordingly, this study used non-targeted lipidomics and transcriptomics to analyze the lipid profiles and metabolism of longissimus dorsi muscle (LDM) and VAT from donkeys. A total of 1,146 and 1,134 lipids belonging to 18 subclasses were identified in LDM and VAT, respectively, with LDM having higher glycerophospholipid (GP) and lower glycerolipid (GL)contents. Polyunsaturated fatty acids (PUFAs) were distributed preferentially at the sn-1 positions in triglycerides (TGs), and sn-2 positions in phosphatidylcholine (PC) and phosphatidylethanolamine (PE). The percentage PUFA content in TGs was significantly lower in LDM than in VAT, while the opposite trend was observed for PUFAs in PC and PE. A total of 110 different lipid molecules (72downregulated and 38upregulated) were identified in LDM compared with VAT, of which 11 were considered potential lipid markers. These different lipids were involved in 17 metabolic pathways, including GLand GP metabolisms. Of the 578 differentially expressed genes screened, 311 were downregulated and 267 were upregulated in LDM compared with VAT. Enriched ontology analysis of the differentially expressed genes mainly involved sphingolipid signaling pathways, and GP, GL, and sphingolipid metabolisms. Overall, lipidomics and transcriptomics indicated differences in lipid profiles and metabolism in LDM and VAT, providing new perspectives for the study of heterogeneity in IMF and VAT.

Keywords

Dezhou Donkey; Lipidomics; Transcriptomics; Heterogeneity; Intramuscular Fat; Visceral Adipose Tissue

Introduction

Meat products are important sources of fat in the human diet globally, with the fat content playing a key role in the overall

palatability of meat. Intramuscular fat (IMF) positively affects the quality and nutritional value of meat, including juiciness, flavor, tenderness, and fatty acid profiles [1,2]. IMF is mainly composed of triglycerides (TGs) and phospholipids, and is rich in phospholipids, palmitic acid, stearic acid, oleic acid, and polyunsaturated fatty acids (PUFA) compared with other adipose tissues, such as visceral adipose tissue (VAT) [3,4]. The differences in IMF and VAT deposition reflect the heterogeneity of the lipidome, especially lipid molecules including glycerophospholipids (GPs) and sphingolipids (SLs), which is unclear.

Recently, to improve meat quality, improving the IMF content of livestock and poultry, and determining the internal molecular mechanisms involved, have become hot topics in genetics, nutrition, and other fields. Previous studies have suggested that the IMF content varies widely depending on animal breed or genetics, slaughter age and weight, nutrition levels, and other factors [5-7]. Some candidate genes for IMF deposition have been identified, such as heart and adipocyte fatty acid binding proteins (H-FABP and A-FABP, respectively), fatty acid synthase (FAS), hormone sensitive lipase (HSL), lipoprotein lipase (LPL), and peroxisome proliferator-activated receptor (PPAR) [8]. Lipid deposition is a process essentially comprising pathways for the synthesis of TGs and GPs from esterified fatty acids of the glycerol skeleton, which are catalyzed by a series of enzymes, including glycerol-3-phospholipid transferase (GPAT), acylglycerol-3-phosphate transferase (AGPAT), and diacylglyceryl transferase (DGAT) in the TG pathway, and choline phosphate transferase (CHPT), ethanolaminephosphate transferase (EPT), and lysophosphatidylcholine transferase (LPCAT) in the GP pathway [9]. DGAT is the rate-limiting enzyme in TG synthesis and has been identified as a candidate gene for IMF deposition [10]. Furthermore, AGPAT has been reported to play a key role in fatty acid deposition and is a key regulatory factor of lipid metabolism in muscle [11]. These findings indicate that genes involved in TG and GP metabolisms in muscle play important roles in regulating IMF deposition.

In recent decades, lipidomics has been successfully applied in various fields to analyze exquisite changes in lipids at the molecular level, especially in food and nutrition science [12]. Many studies have used lipidomics to clarify lipid profile changes in donkey milk during lactation [13] and egg yolk in different diets [14], and differentiate domestic pork [15], and chicken [16]. A recent study reported the transcriptome atlas of 16 Dezhou Donkey tissues [17].However, few studies have used lipidomics to analyze differences between IMF and VAT. Therefore, the present study used liquid chromatography–mass spectrometry (LC-MS)-based lipidomics detection of IMF and VAT from donkey to analyze differences in the amounts, classes, fatty acid distributions, and metabolism pathways of lipids. Furthermore, transcriptomics analysis was used to analyze differentially expressed genes and their functional enrichment in IMF and VAT. Subsequently, IMF and VAT were distinguished at the lipid molecular level and key regulating pathways were determined by combining lipidomics and transcriptomics. This study investigated the heterogeneity of IMF and VAT at the molecular level, and provides a new perspective for understanding and improving IMF content.

Materials and Methods

Animal and Sample Collection

All experimental procedures involving donkeys were approved by the Liaocheng University Animal Care and Use Committee. Thirty-six male Dezhou donkeys, ~18 months old and of similar weight (150±20 kg), were randomly divided into three groups of 12 donkeys each. All donkeys were fed a diet of 70% silage corn straw and 30% corn flour, and were free to eat and drink under the same living conditions. The experiment was conducted at a local farm in Liaocheng City, Shandong Province, China for six months.

After the experiment, all donkeys were left unfed for 12 h and weighed (230±31 kg). Three donkeys from each group were randomly selected and transported to Shandong Dong'e Tianlong Food Co., Ltd.. After slaughter, LDM and VAT samples were

collected, immediately snap frozen in liquid nitrogen, and stored at -80 °C for lipidomic and transcriptomic analysis.

Lipid Extraction and Lipidomic Assay

Muscle samples were ground with chloroform/methanol (2:1, *v/v*)using a Xinzhi high-flux tissue grinder (Ningbo, China) at 4 °C. Lipids were extracted on ice for 3h, centrifuged at 8,000 ×g for 20 min at 4 °C, and the resultant supernatant was concentrated to dryness under vacuum. The lipids were then dissolved in isopropanol (200 μL) and stored at −80 °C for subsequent analysis.

LC-MS was performed according to published methods [18]. LC-MS analysis was performed on a AB SCIEX Triple TOF 6600 plus MS (AB SCIEX Inc, Massachusetts, USA) coupled to a UHPLC Nexera Agilent 1290 (Agilent Technologies, Palo Alto, CA, USA) equipped with a Phenomenex Kinetex C18 column (1.7 μm, 100×2.1 mm, Agilent). The lipid samples were redissolved in 90% isopropanol/acetonitrile (200 μL) and filtered through a 0.22-μm polyvinylidene fluoride membrane, with 2 and 62 μL of each sample injected for analysis in positive and negative modes, respectively. The auto sampler and column temperatures were maintained at 8 °C and 55 °C, respectively. Solvents A and B were acetonitrile/water (60:40, *v/v*) and isopropanol/acetonitrile (90:10, *v/v*), respectively, each containing 0.1% formic acid and 10 mM ammonium formate. Gradient elution was performed using the following mobile phase compositions: 40% solvent B at a flow rate of 0.3 mL/min at 0–1.5 min; increased to 85% solvent B at 1.5–10.5 min; equilibration with 85% solvent B at 10.5–14 min; increased to 100% solvent B at 14–14.1 min; equilibration with 100% solvent B at 14.1–15 min; decreased to 40% solvent B at 15–15.2 min; and finally equilibration with 40% solvent B at 15.2–18 min. To avoid instrumentation error, quality control (QC) samples were prepared by mixing all samples. QC samples were inserted into the detection queue to monitor and evaluate stability and reliability during the experiment.

After LC separation, an AB SCIEX Triple TOF 6600 plus MS was used to measure mass-to-charge ratios (*m/z*).The atomization gas, auxiliary gas, and air curtain gas pressures were 60,60,and 30 psi, respectively, the temperature was 600°C, and the positive mode, negative mode, and declustering potentials of the ion source were 5, –4.5, and 0.1 kV, respectively. Data acquisition was performed by tandem mass spectrometry (MS/MS), involving a rapid time-of-flight (TOF) MS survey scan. For the TOF MS survey scan, the scanning ranges of positive and negative ion modes were *m/z* 200–2000 and 100–2000, respectively. After each scan, ten fragment patterns (MS2 scan, HCD) were collected to obtain the *m/z* ratios of lipid molecules to lipid fragments. Dynamic background subtraction was applied and the dynamic exclusion method was used to remove noise in MS/MS spectra. Raw data were annotated based on the Lipid Structure Database (LMSD; http://www.lipidmaps.org/) and assessed by orthogonal partial least squares discriminant analysis (OPLS-DA). Lipid species with a variable importance in projection (VIP) of >1 and *p*-value of <0.05 were identified as statistically significant. The Kyoto Encyclopedia of Genes and Genomes (KEGG) pathway database (https://www.kegg.jp/kegg/) was used to search for enriched metabolites and pathways related to differential lipid molecules.

RNA-Seq Analysis

RNA-seq analysis was performed as previously reported[19]. Total RNA extraction and RNA-seq analysis were performed by Shanghai Majorbio Bio-pharm Technology Co., Ltd (Shanghai, China). Briefly, total RNA was extracted from the samples using Trizol reagent (Takara, China).Subsequently, double-stranded cDNA was synthesized by a specific kit (Invitrogen, CA) with random hexamer primers (Illumina). The as-synthesized cDNA was subjected to end-repair, phosphorylation, and 'A' base addition sequentially. The cDNA target fragments of 200–300 bp were selected on 2% low range ultra agarose with subsequent PCR amplification. RNA-seq libraries were sequenced in a single lane using an Illumina Novaseq 6000 sequencer (Illumina, San Diego, CA). High-quality sequences (clean reads) were obtained by removing low-quality sequences and connect or

contamination from the raw reads sequenced using SeqPrep software (https://github.com/jstjohn/SeqPrep).The clean reads were de novo assembled using Trinity software (https://github.com/trinityrnaseq/trinityrnaseq) without a reference genome. To annotate the transcriptome, six databases, including the National Center for Biotechnology Information NR database (hftp://ftp.ncbi.nlm.nih.gov/blast/db/), Swiss-Prot protein database (http://web.expasy.org/docs/swiss-prot_guideline.html), Pfam database (http://pfam.xfam.org/), Clusters of Orthologous Groups (COG) of proteins database (http://www.ncbi.nlm.nih.gov/COG/), Gene Ontology (GO) database (http://www.geneontology.org), and KEGG database were searched using BLAST with a cut-off e-value of 10^{-5}. Gene expression was given infragments per kilobase per million mapped fragments (FPKM) using DESeq2. Genes expressed differentially in LDM and VAT were screened using DESeq2. Genes with $p<0.05$ and $|\log2(\text{foldchange})| > 1.5$ were identified as statistically significant.

Statistical Analysis

Data were presented asmeans ± standard error of the mean (SEM), and analyzed by one-way analysis of variance (ANOVA), followed by Tukey's test for pairwise comparisons using SPSS 26.0 software (SPSS Inc., Chicago, IL, USA). $p<$ 0.05 was considered statistically significant

Results

Lipid Profiles

As shown in Figures 1A and 1B, qualitative lipid analysis achieved excellent separation for IMF and VAT. The OPLS-DA scores were $R^2X = 0.863$, $R^2Y = 0.993$, and $Q^2 = 0.892$ in positive and negative ion modes, and corresponding OPLS-DA validation plots were applied, providing R^2 and Q^2 intercept parameters of (0.0, 0.63) and (0.0, -0.11), respectively (Figures S1A and S1B). A total of 1,146 and 1,134 lipids, belonging to 18 subclasses, were identified in donkey LDM and VAT, respectively, mainly comprising glycerolipids (GLs), GPs, and SLs (Figures 1C and 1D). The relative contents of TGs and

diacylglycerol (DG) in LDM were significantly lower than those in VAT ($p< 0.001$), while the contents of phosphatidylcholine (PC), phosphatidylethanolamine (PE), phosphatidylglycerol (PG), phosphatidylinositol (PI), phosphatidylserine (PS), phosphatidic acid (PA), lysophosphatidylcholine (LPC), lysophosphatidylethanolamine (LPE), lysophosphatidylglycerol (LPG), and sphingomyelin (SM) in LDM were significantly higher than those in VAT ($p< 0.001$) (Figure 1E). The relative ceramide (Cer) contents showed no significant difference between the two groups ($p> 0.05$).

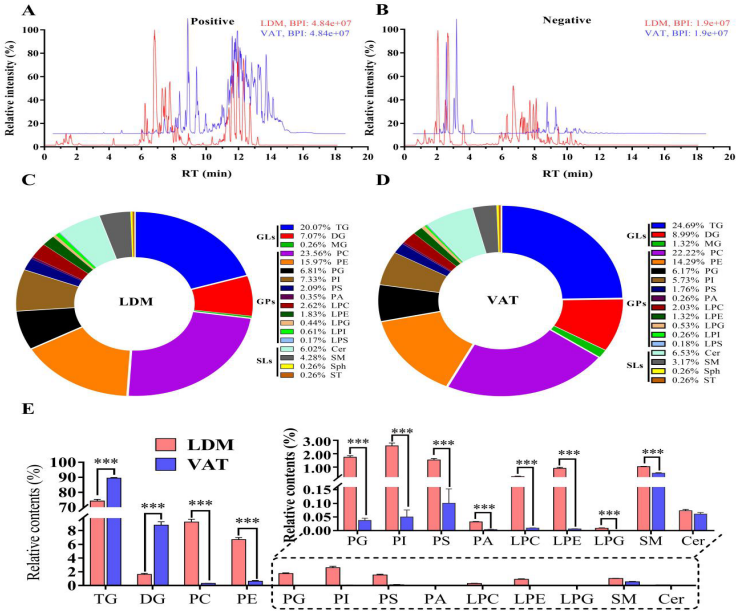

Figure 1: Overall lipid composition and content in LDM and VAT of Dezhou donkey. (A,B) Representative base peak diagrams of electrospray ionization in (A) positive and (B) negative modes. (C,D) Percentage of lipid subclasses in (C) LDM and (D) VAT. (E) Relative lipid content (% total lipids) in LDM and VAT of Dezhou donkey. Values are presented as means ± SEM (n = 9), ***$p< 0.001$.

Positional Distribution of Fatty Acids

As shown in Figure 2, the percentage contents of saturated fatty acid (SFAs) (12:0, 14:0, 16:0, and 18:0) in TGs were higher at the sn-3 position than that at the sn-1 and sn-2 positions, while the percentage contents of SFAs in PC and PE were higher at the sn-1 position. Furthermore, the percentages of 16:0 at the sn-2 and sn-3 positions in TGs, and the sn-1 and sn-2 positions in PC, and 14:0 at the sn-3 positions in TGs were significantly higher in LDM than in VAT ($p< 0.001$). In contrast, the percentages of 18:0 at the two positions in PC and PE were significantly lower in LDM than in VAT ($p< 0.001$).

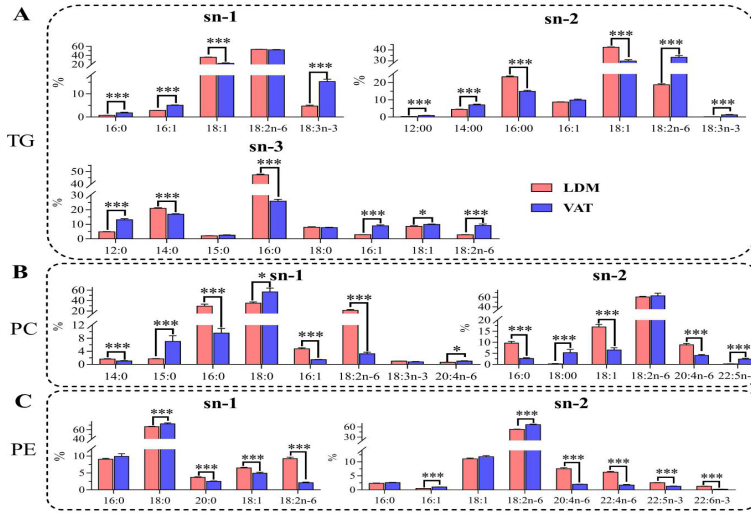

Figure 2: Positional distributions (sn-1, sn-2, and sn-3) of fatty acids in (A) TGs, (B) PC, and (C) PE in LDM and VAT of Dezhou donkey. Values are presented as means ± SEM (n = 9), *$p< 0.05$, ***$p< 0.001$. TG, triglyceride; PC, phosphatidylcholine; PE, phosphatidylethanolamine.

The percentage contents of monounsaturated fatty acid (MUFAs) (16:1 and 18:1) at the sn-2 positions of TGs, PC, and PE were higher than those at the sn-1 or sn-3 positions. The percentage contents of 18:1 at the sn-1 and/or sn-2 positions of TGs, PC, and PE were significantly higher in LDM than in VAT ($p< 0.001$), while the percentage contents of 16:1 and 18:1 at the sn-3 positions of TGs were higher in VAT than in LDM ($p<0.05$).

The distributions of PUFAs (18:2n-6, 18:3n-3, and 20:4n-6) were higher at the sn-1 position in TGs, and at the sn-2 positions in PC and PE. Furthermore, the percentage contents of 18:2n-6 at the sn-2 and sn-3 positions in TGs, and the sn-2 position in PE, were significantly lower in LDM than in VAT, while percentage contents of 18:2n-6 at the sn-1 position in PC were higher in VAT than in LDM ($p< 0.001$). The percentage contents of 18:3n-3 at the sn-1 and sn-2 positions in TGs were significantly lower in LDM than in VAT ($p<0.001$), while the percentage contents of 20:4n-6, 22:4n-6, 22:5n-3, and 22:6n-3 at the sn-1 and sn-2 positions in PC and PE were significantly higher in VAT than in LDM ($p<0.001$).

Differential Lipid Molecules and Potential Lipid Markers

As shown in Figure S2, 110 lipids were identified as differential lipid molecules, of which 72 were downregulated and 38 were upregulated in LDM compared with VAT. These differential lipid molecules comprised 4 LPEs, 16 PCs, 8 PEs, 4 PGs, 4 PIs, 1 PS, 3 SMs, 7 DGs, and 63 TGs (Table S1; $|\log2(\text{Fold Change})| >1$; VIP >1; $p<0.05$). The 72 downregulated lipids comprised 7 DGs, 63 TGs, and 2 SMs, while the 38 upregulated lipids comprised 4 LPEs, 16 PCs, 8 PEs, 4 PGs, 4 PIs, 1 PS, and 1 SM (Figures 3A–3D).

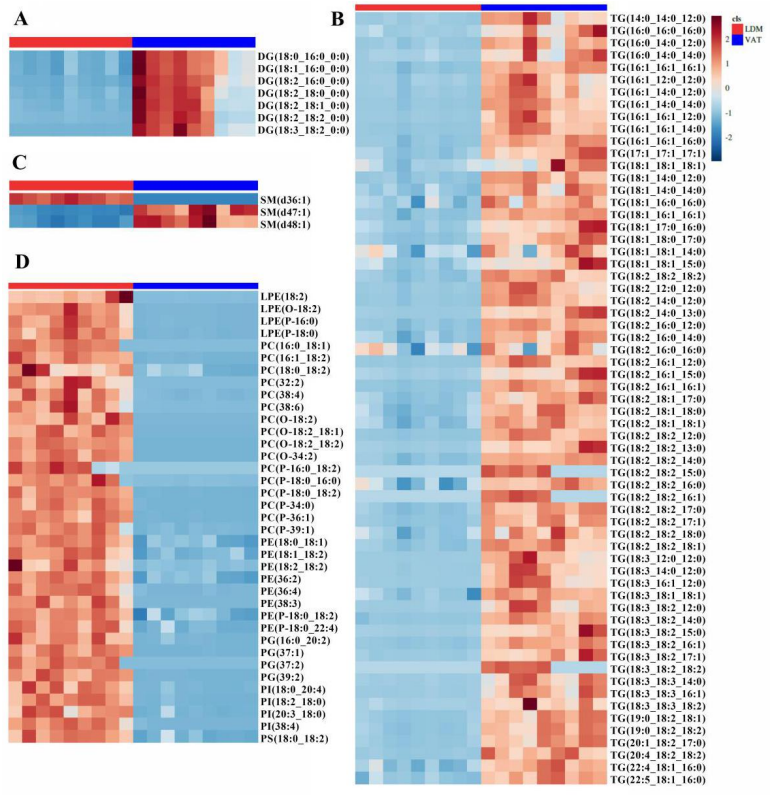

Figure 3: Difference in lipid molecules of donkey LDM and VAT. Heatmap analysis of (A) DG, (B) TG, (C) SP, and (D) GP molecules. Colors indicate decreased (blue band) or increased (red band) levels of lipid molecules in LDM vs. VAT. DG, diacylglycerol; TG, triglyceride; SP, sphingolipids; GP, glycerophospholipids.

Figure 4A and Table S2 showed the receiver operating characteristic (ROC) curves and parameters for the top 11 discriminating lipids, with an area under the ROC curve (AUC) of 1, specificity of 100%, and sensitivity of 100% for PC(O-18:2/18:2), PC(O-18:2/18:1), PC(32:2), PC(O-18:2), PC(38:6), PE(38:3), LPE(O-18:2), PG(37:2), PG(39:2), PI(38:4), and SM(d36:1). These potential lipid markers comprised 5 PCs, 2 PEs, 2 PGs, 1 PI, and 1 SM, for which the normalized intensity was significantly higher in LDM than in VAT, and close to 0 in VAT (Figures 4B–4F).

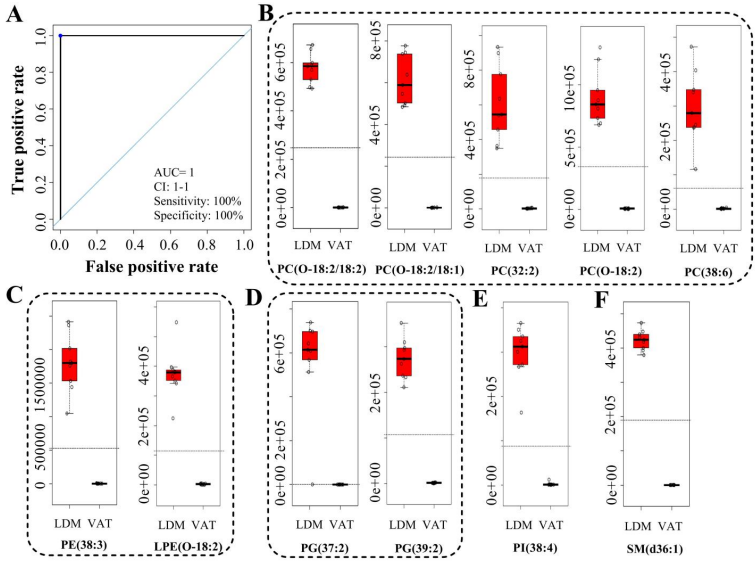

Figure 4: Receiver operating characteristic curve and normalized intensity for potential lipid markers. (A) Receiver operating characteristic curve of (B–F). (B–F) Normalized intensity for potential lipid markers in LDM and VAT. AUC is the area under the ROC curve; CI 1-1 is the lower and upper limit of the AUC confidence interval.

Lipid Metabolism Pathways

Functional enrichment analysis was conducted on the 110 lipids showing significant differences between LDM and VAT using the KEGG pathways. This revealed significant enrichment of 17 major metabolic pathways, including arachidonic acid metabolism, GP metabolism, α-linolenic acid metabolism, vitamin digestion and absorption, GL metabolism, and linoleic acid metabolism (Figure 5A). Cholesterol metabolism, fat digestion and absorption, lipolysis regulation in adipocytes, GP metabolism, GL metabolism, thermogenesis, linoleic acid metabolism, arachidonic acid metabolism,linolenic acid metabolism, vitamin digestion and absorption, insulin resistance, and glycosylphosphatidylinositol-anchor biosynthesis were the most relevant metabolic pathways, as shown in Figure 5B. GL and GP metabolisms are shown in Figure 5C. The expression of DG and TGs by GL metabolism was significantly lower in LDM

than in VAT ($p< 0.05$), while the expression of PC, PE, PS, PG, and LPE by GP metabolism was significantly lower in VAT than in LDM ($p< 0.05$).

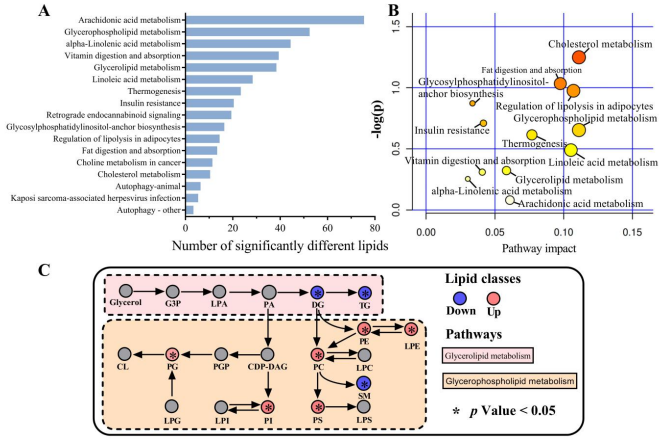

Figure 5: Metabolic pathways involved in different lipid species of LDM and VAT. (A) Kyoto Encyclopedia of Genes and Genomes (KEGG) enrichment pathways of significantly different lipids in LDM compared with VAT. (B) Map of significant metabolic pathways in LDM compared with VAT.(C) Enrichment of significantly different lipids in glycerol lipid metabolism and glycerophospholipid metabolism in LDM compared with VAT.

Gene Expression in Lipid Metabolic Pathways

As shown in Table S3, 55,118,7981,721,661 and 56,402,6561,200,757 clean reads were obtained in LDM and VAT, respectively. After de novo assembly, 154,948,346 unigenes were obtained, with the GC percentage reaching 47.02%. The clean reads were matched with the corresponding assembly sequences, and the BUSCO score was 82.30%. The 138,936 assembled unigenes were annotated by the BLAST tool using six public databases. Among them, 20,587 (14.82%), 20,300 (15.61%), 24,000 (17.27%), 39,202 (28.22%), 26,119 (18.80%), and 17,537 (12.62%) unigenes were matched with the GO, KEGG, COG, NR, Swiss-Prot, and Pfam databases, respectively. A total of 40,696 (29.29%) unigenes were annotated in six public databases.

A total of 578 differentially expressed genes were identified, of which 311 were downregulated and 267 were upregulated in LDM compared with VAT (Figure 6A). RNA-seq analysis showed that the expression of GL metabolism-related genes and GP metabolism-related genes, including glycerol kinase (GK), glycerol-3-phosphate acyltransferases 1 and 3 (GPAT1, GPAT3), 1-acylglycerol-3-phosphate O-acyltransferases 2 and 8 (AGPAT2 and AGPAT8), LPIN1 and LPIN2, diacylglycerol O-acyltransferases 1 and 2 (DGAT1 and DGAT2), and cytidylyltransferases 1 and 2 (CDS1 and CDS2), was significantly downregulated in LDM compared with VAT. Meanwhile, the expression of GPAT2, AGPAT1, AGPAT3, AGPAT4, AGPAT5, AGPAT7, phosphatidylglycerol 3-phosphatidyltransferase (PGS1), cholinephosphotransferase 1 (CHPT1), choline/ethanolaminephosphotransferase 1 (CEPT1), phospholipase (PLA), phosphatidylethanolamine N-methyltransferase (PEMT), lysophosphatidylcholineacyltransferases 1 and 2 (LPCAT1 and LPCAT2), and lysophosphatidylglycerolacyltransferase (LPGAT1) was significantly upregulated in LDM compared with VAT (Figure 6B). KEGG enrichment analysis of the differentially expressed genes showed that genes regulating GL, GP, and sphingolipid metabolisms, and fatty acid degradation, were enriched (Figure 6C). Functional enrichment analysis of GL and GP metabolisms conducted using the KEGG pathways showed that the expression of GL metabolism-related genes was significantly decreased in LDM compared with VAT ($p<0.05$), while the expression of GP metabolism-related genes was significantly increased in LDM compared with VAT ($p<0.05$), as shown in Figure 6D.

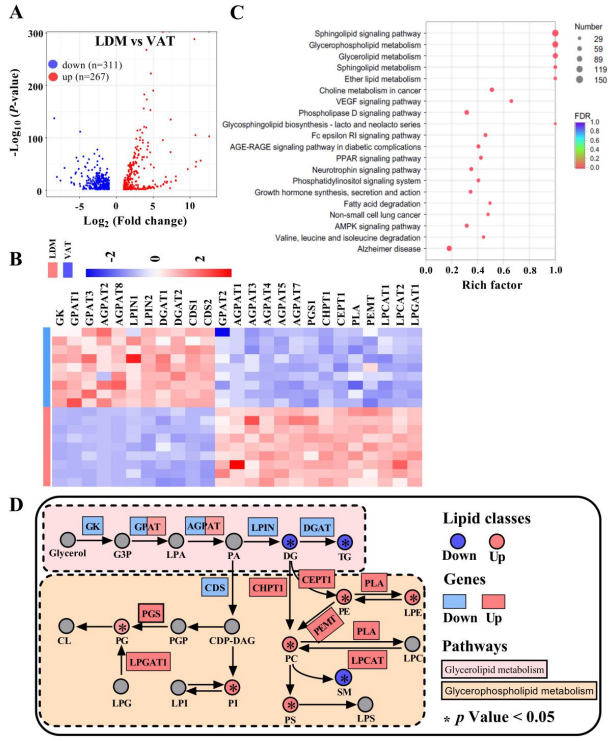

Figure 6: Expression of lipid metabolism-related genes in LDM and VAT. (A) Differential expressed genes between LDM and VAT. (B) Heatmap of relative expression of selected major lipid metabolism-related genes in LDM compared with VAT. (C) KEGG enrichment pathways of different lipid metabolism-related genes in LDM compared with VAT. (D) Selected glycerolipid and glycerophospholipid metabolisms reactions from KEGG, with indications of lipid classes and genes significantly regulated in LDM compared with VAT.

Discussion

In contrast to traditional approaches, LC-MS-based lipidomics allows simultaneous identification and quantification of more than 1,000 lipid molecules, which directly clarifies the interrelation between phenotype and mechanism [20]. The heterogeneity of IMF and VAT was elucidated using lipidomics analysis, which provides better understanding of the muscle nutritional value and improve IMF content. In the present study, 1,146 and 1,134 lipids were identified in LDM and VAT,

respectively, comprising 18 subclasses. These results were consistent with the 1,180 and 1,127 lipid species found in pork [15] and chicken [16], respectively, and significantly higher than found in donkey milk (335 lipids species) (13) in previous studies. Furthermore, the number and relative content of GPs (such as PC, PE, PG, PI, and PS) and SL (SM)were significantly higher in LDM than in VAT. These findings further confirmed that IMF was rich in lipid classes, especially phospholipid classes [4]. Furthermore, TGs were identified as the predominant lipid class in LDM, followed by PC and PE, which were selected for more intensive analysis.

In the present study, the SFAs (14:0, 16:0, and 18:0)in donkey muscle were distributed preferentially at the outer positions of the glycerol backbone in predominant lipid classes (sn-3 positions of TG molecules and sn-1 positions of PC and PE molecules). These results were in agreement with those reported for Nile tilapia fillet [21]. However, 16:0 is distributed preferentially at the sn-2 position in breast, bovine milk, and lard, which are easily digested and absorbed by humans, with an excess intake of 16:0 at the sn-2 position of lipids potentially increasing the risk of obesity and atherogenesis [22,23]. In contrast, 16:0 at the sn-1/3 positions of lipids are selectively lipolyzed by pancreatic lipase [24]. This result suggested that, after human consumption, SFAs in donkey meat are easily mobilized and consumed, reducing the chance of fat storage and risk of cardiovascular and cerebrovascular diseases, hypertension, and obesity in humans. In this study, 18:1 fatty acids were esterified preferentially at the 2-position of TGs, PC, and PE. This result was consistent with previously reported 18:1 fatty acids in vegetable and animal (most nonmilk) lipids [25]. The percentage contents of 18:1 in TGs, PC, and PE in LDM were significantly higher than those in VAT. As 18:1 has the ability to remove bad cholesterol and protect cardiovascular and cerebrovascular health in human nutrition [26], the nutritional value of donkey meat needs further investigation. This result suggested that donkey meat is a good source of 18:1 for human consumption.

The present study showed that PUFAs were preferentially deposited at the sn-1 positions in TGs, and the sn-2 positions in PC and PE. Regarding nutrition, 18:2n-6 at the sn-1/3 positions is more likely to be released from TGs into the circulation system, and might increase the risk of inflammation [27]. A recent study showed that, in fish fed with perilla oil and fish oil enriched with n-3 PUFAs, the levels of 18:2n-6 at the sn-2 position in TGs in the fillets was increased compared with those fed with palm oil, olive oil, and safflower oil [21], indicating that the positional distribution of 18:2n-6 in TGs was affected by dietary oils. In PC and PE molecules, PUFAs were preferentially deposited at the sn-2 position, which is generally consistent with previous studies, and is relatively stable and better retained to play roles in important functions [25,28]. Furthermore, the PUFA levels in PC and PE were significantly higher in LDM than in VAT. These results further demonstrated that IMF was rich in PUFAs, especially at the sn-2 position.

In the present study, the difference between IMF and VAT at the lipid molecular level was mainly manifested in GPs (PC, PE, LPE, PG, PI, PS) and GLs (DG and TG), with IMF rich in GPs and VAT rich in GLs. This result was consistent with a previous report, which showed that the LDM of pigs contains a large GP content and upregulated PUFAs [29]. The heterogeneity of lipid profiles in IMF and VAT could be associated with cell type and fat deposition rates [30]. GPs, which show significant differences among different types of cell, are the main components of cell membrane, where they play key roles, such as providing structural attributes and signaling processes [31,32]. IMF was rich in GPs due to originating from muscle cells and adipocytes, while VAT only originated from adipocytes. Furthermore, IMF exhibits smaller adipocyte diameters and lower adipose maturation compared with VAT [33]. A higher proportion of energy is available for fat in muscle, and the fat content of IMF (only 2%–5% on average) might be lower than in other adipose tissues [34]. In this study, the above lipids were enriched in 17 metabolic pathways. According to the degree of impact on the metabolic pathway, GL and GP metabolisms were key metabolic pathways regulating lipid deposition. This result was similar to the findings reported for IMF deposition in pork [29]. This was

further supported by the GLs and GPs of significantly different lipids being mostly synthesized by the TG and GP pathways [9].

Lipid accumulation can be regulated by transcription, leading to different lipid profiles in tissues [35]. Previous studies have shown that the differential deposition of IMF in pork might be caused by differences in fatty acid, GL, and GP metabolism pathways [29,36].In the present study, the transcriptome results showed that, among a total of 578 differentially expressed genes were screened, the expression of GL metabolism-related genes was significantly downregulated in LDM compared with VAT, while the opposite trend was observed for the expression of GP metabolism-related genes. Furthermore, functional enrichment analysis revealed the differentially expressed genes involved in the GL and GP metabolism, and PPARs and AMPK signaling pathways. These findings indicated that the GL and GP metabolism pathways were key pathways in regulating IMF at the molecular level. Indeed, this was supported by the lipid being mainly composed of TGs, and phospholipids being synthesized by the GL and GP pathways [9].

Conclusion

This study analyzed lipid profiles and metabolism in IMF and VAT from donkeys using nontargeted lipidomics and transcriptomics. A total of 1,146 and 1,134 lipids were identified in LDM and VAT, respectively. Donkey IMF is rich in GPs and PUFAs distributed preferentially at the sn-1 positions of TGs and sn-2 positions of PC and PE. This phenotype might result from the higher content of 38lipid molecules (37 GPs and 1 SM) and the expression of lipid synthesis-related genes in IMF. GL and GP metabolisms were considered key IMF-regulating pathways. These results provide new perspectives for understanding the heterogeneity of IMF and VAT, and developing new strategies to regulate IMF deposition.

References

1. Frank D, Joo S, Warner R. Consumer acceptability of intramuscular fat. Korean J Food Sci an. 2016; 36: 699-708.

2. Listrat A, Lebret B, Louveau I, Astruc T, Bonnet M, et al. How muscle structure and composition influence meat and flesh quality. Sci World J. 2016; 2016: 3182746.
3. Hou B, Zhao Y, He P, Xu C, Ma P, et al. Targeted lipidomics and transcriptomics profiling reveal the heterogeneity of visceral and subcutaneous white adipose tissue. Life Sci. 2020; 245: 117352.
4. Zhang J, Yu Y, Shen Y, Zhao Y, Guo X, et al. Distribution of fatty acid and cholesterol content in muscle and adipose tissue of donkey. Feed Research. 2021; 92-97.
5. Tyra M, Ropka-Molik K, Terman A, Piórkowska K, Oczkowicz M, et al. Association between subcutaneous and intramuscular fat content in porcine ham and loin depending on age, breed and FABP3 and LEPR genes transcript abundance. MolBiol Rep. 2013; 40: 2301-2308.
6. Jin C, Wang Q, Zhang Z, Xu Y, Yan H, et al. Dietary supplementation with pioglitazone hydrochloride and chromium methionine improves growth performance, meat quality, and antioxidant ability in finishing pigs. J Agr Food Chem. 2018; 66: 4345-4351.
7. Frank D, Ball A, Hughes J, Krishnamurthy R, Piyasiri U, et al. Sensory and flavor chemistry characteristics of australian beef: Influence of intramuscular fat, feed, and breed. J Agr Food Chem. 2016; 64: 4299-4311.
8. Maryam A, Jae Myoung S, Nasun H, Christopher L, Atkins AR, et al. PPARγ signaling and metabolism: The good, the bad and the future. Nat Med. 2013; 19: 557-566.
9. Atsushi Y, Yasuhiro H, Naoki M, Yoko NS, Saori O, et al. Glycerophosphate/Acylglycerophosphateacyltransferases. Biology. 2014; 3: 801-830.
10. Shi, Cheng Y. Beyond triglyceride synthesis: The dynamic functional roles of MGAT and DGAT enzymes in energy metabolism. Am J Physiol-Endoc M. 2009; 297: 10-18.
11. Takeuchi K, Reue K. Biochemistry, physiology, and genetics of GPAT, AGPAT, and lipin enzymes in triglyceride synthesis. Am J Physiol-Endoc M. 2009; 296: 1195-1209.
12. Sun T, Wang X, Cong P, Xu J, Xue C. Mass spectrometry-based lipidomics in food science and nutritional health: A comprehensive review. Compr Rev Food Sci F. 2020; 19: 2530-2558.

13. Li M, Li W, Wu J, Zheng Y, Shao J, et al. Quantitative lipidomics reveals alterations in donkey milk lipids according to lactation. Food Chem. 2020; 310: 125866.
14. Wu B, Xie Y, Xu S, Lv X, Yin H, et al. Comprehensive lipidomics analysis reveals the effects of different omega-3 polyunsaturated fatty acid-Rich diets on egg yolk lipids. J Agr Food Chem. 2020; 68: 15048-15060.
15. Mi S, Shang K, Li X, Zhang C, Liu J, et al. Characterization and discrimination of selected China's domestic pork using an LC-MS-based lipidomics approach. Food Control. 2019; 100: 305-314.
16. Mi S, Shang K, Jia W, Zhang C, Li X, et al. Characterization and discrimination of Taihe black-boned silky fowl Gallus gallusdomesticus Brisson; muscles using LC/MS-based lipidomics. Food Res Int. 2018; 109: 187-195.
17. Wang Y, Miao X, Zhao Z, Wang Y, Li S, et al. Transcriptome atlas of 16 Donkey tissues. Front Genet. 2021; 12: 1458.
18. Triebl A, Trötzmüller M, Hartler J, Stojakovic T, Köfeler HC. Lipidomics by ultrahigh performance liquid chromatography-high resolution mass spectrometry and its application to complex biological samples. JChromatogrB. 2017; 1053: 72-80.
19. Lei CX, Li MM, Tian JJ, Wen JK, Li YY. Transcriptome analysis of golden pompano Trachinotusovatus; liver indicates a potential regulatory target involved in HUFA uptake and deposition. Comp Biochem Phys D. 2020; 33: 100633.
20. Li J, Zhang J, Yang Y, Zhu J, He W, et al J. Comparative characterization of lipids and volatile compounds of Beijing Heiliu and Laiwu Chinese black pork as markers. Food Res Int. 2021; 146: 110433.
21. Liu Y, Jiao JG, Gao S, Ning LJ, Mchele Limbu S, et al Y. Dietary oils modify lipid molecules and nutritional value of fillet in Nile tilapia: A deep lipidomics analysis. Food Chem. 2019; 277: 515-523.
22. Kubow S. The influence of positional distribution of fatty acids in native, interesterified and structure-specific lipids on lipoprotein metabolism and atherogenesis. J Nutr Biochem. 1996; 7: 530-541.

23. Jiang T, Liu B, Li J, Dong X, Lin M, et al. Association between sn-2 fatty acid profiles of breast milk and development of the infant intestinal microbiome. Food Funct. 2017; 9: 1028–1037.
24. Lien EL. The role of fatty acid composition and positional distribution in fat absorption in infants. J Pediatr. 1994; 125: S62-S68.
25. Small DM. The effects of glyceride structure on absorption and metabolism. Annu Rev Nutr. 1991; 11: 413-434.
26. Romani A, Ieri F, Urciuoli S, Noce A, Marrone G, et al. Health effects of phenolic compounds found in Extra-Virgin olive oil, By-Products, and leaf of oleaeuropaea l. Nutrients. 2019; 11: 1776.
27. Naughton SS, Mathai ML, Hryciw DH, McAinch AJ. Linoleic acid and the pathogenesis of obesity. Prostag Oth Lipid M. 2016; 125: 90-99.
28. Ruizlopez N, Stubhaug I, Ipharraguerre I, Rimbach G, Menoyo D. Positional distribution of fatty acids in triacylglycerols and phospholipids from fillets of atlantic salmon Salmosalar; fed vegetable and fish oil blends. Mar Drugs. 2015; 13: 4255-4269.
29. Zhang Z, Liao Q, Sun Y, Pan T, Liu S, et al. Lipidomic and transcriptomic analysis of the longissimus muscle of luchuan and duroc pigs. Front Nutr. 2021; 8: 667622-667622.
30. Zhao J, Li K, Yang Q, Du M, Liu X, et al. Enhanced adipogenesis in Mashen pigs compared with Large White pigs. Ital J Anim Sci. 2017; 16: 217-225.
31. Wood JD, Enser M, Fisher A V, Nute GR, Sheard PR, et al. Fat deposition, fatty acid composition and meat quality: A review. Meat Sci. 2008; 78: 343-358.
32. Yen CE, Nelson DW, Yen M. Intestinal triacylglycerol synthesis in fat absorption and systemic energy metabolism. J Lipid Res. 2015; 56: 489-501.
33. Franco I, Cristina Escamilla M, García J, Camino García Fontán M, Carballo J. Fatty acid profile of the fat from Celta pig breed fattened using a traditional feed: Effect of the location in the carcass. J Food Compos Anal. 2006; 19: 792-799.
34. Monziols M, Bonneau M, Davenel A, Kouba M. Comparison of the lipid content and fatty acid composition

of intermuscular and subcutaneous adipose tissues in pig carcasses. Meat Sci. 2007; 76: 54-60.
35. Poklukar K, Čandek-Potokar M, BatorekLukač N, Tomažin U, Škrlep M. Lipid deposition and metabolism in local and modern pig breeds: A review. Animals. 2020; 10: 424.
36. Damon M, Wyszynska-Koko J, Vincent A, Hérault F, Lebret B. Comparison of muscle transcriptome between pigs with divergent meat quality phenotypes identifies genes related to muscle metabolism and structure. Plos One. 2012; 7: e33763.

Supplementary Materials

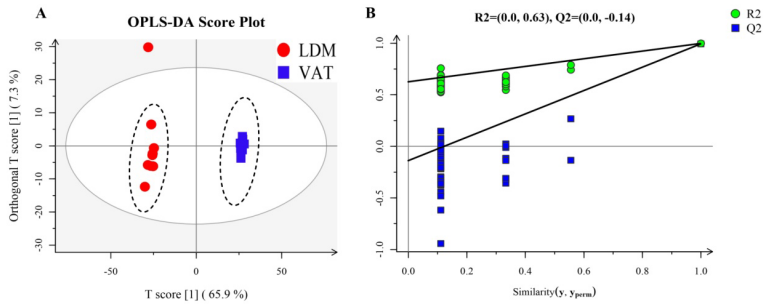

Figure S1: (A) OPLS-DA score plots are based on lipidomic data from intramuscular fat and visceral adipose tissue (R^2X = 0.863, R^2Y = 0.993, Q^2 = 0.892) and (B) corresponding OPLS-DA validation plots (R^2 = (0.0, 0.63), Q^2 = (0.0, -0.11).

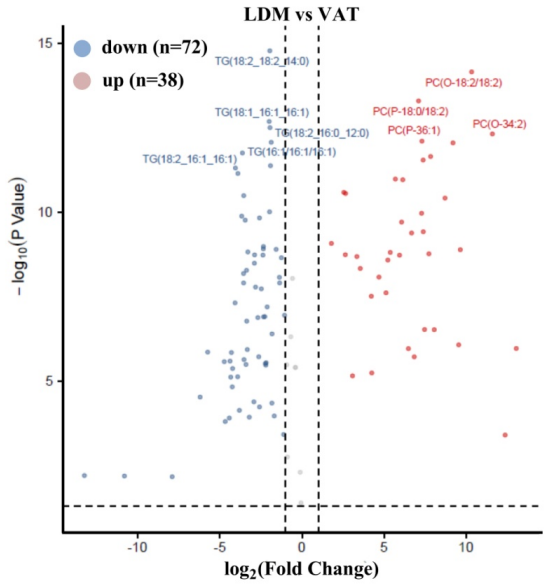

Figure S2: Log_2 (fold changes) in lipid molecule in LDM and VAT and the corresponding significance values displayed as -log10 (*P* value). The transverse and vertical dotted lines indicate the cutoff value for differential expression ($P < 0.05$ and $|Log_2$ (fold changes)$| > 1$). In total, 38 and 72 lipid molecules were identified that had up-regulation (red) or down-regulation (blue) levels in LDM vs. VAT.

Table S1: Information on different lipid molecules in LDM and VAT of Dezhou donkey.

No.	Lipid name	Lipid category	Accurate mass	Rt (s)	Fold Change	log2(FC)	*P* value	FDR	VIP
1	LPE(18:2)	GPs	476.2768	71.2530	88.64	6.47	0.0000	0.0000	1.26
2	LPE(O-18:2)	GPs	462.2978	100.5735	165.91	7.37	0.0000	0.0000	1.50
3	LPE(P-16:0)	GPs	436.2826	95.8190	101.29	6.66	0.0000	0.0000	1.10
4	LPE(P-18:0)	GPs	464.3132	132.1655	66.51	6.06	0.0000	0.0000	1.33
5	PC(16:0_18:1)	GPs	804.5573	401.1870	740.04	9.53	0.0000	0.0000	1.62
6	PC(16:1_18:2)	GPs	800.5363	362.6660	69.91	6.13	0.0000	0.0000	1.13
7	PC(18:0_18:2)	GPs	830.5805	463.2205	8.39	3.07	0.0000	0.0000	2.36
8	PC(32:2)	GPs	730.5302	352.3390	263.53	8.04	0.0000	0.0000	1.87
9	PC(38:4)	GPs	810.5990	423.4610	34.50	5.11	0.0000	0.0000	1.28
10	PC(38:6)	GPs	806.5693	359.7590	175.08	7.45	0.0000	0.0000	1.30
11	PC(O-18:2)	GPs	564.3288	73.7950	210.17	7.72	0.0000	0.0000	2.32
12	PC(O-18:2_18:1)	GPs	814.5854	446.1380	415.07	8.70	0.0000	0.0000	1.94
13	PC(O-18:2_18:2)	GPs	812.5716	437.5335	1273.90	10.32	0.0000	0.0000	1.90
14	PC(O-34:2)	GPs	788.5659	439.9990	3059.40	11.58	0.0000	0.0000	2.39
15	PC(P-16:0_18:2)	GPs	786.5560	430.5520	5237.40	12.36	0.0004	0.0006	2.15
16	PC(P-18:0_16:0)	GPs	790.5844	491.8020	113.30	6.82	0.0000	0.0000	1.15
17	PC(P-18:0_18:2)	GPs	814.5853	493.3990	136.05	7.09	0.0000	0.0000	1.91
18	PC(P-34:0)	GPs	746.5940	446.4045	225.59	7.82	0.0000	0.0000	1.85
19	PC(P-36:1)	GPs	816.6008	505.7020	156.85	7.29	0.0000	0.0000	1.42
20	PC(P-39:1)	GPs	858.6673	540.9930	25.58	4.68	0.0000	0.0000	1.25
21	PE(18:0_18:1)	GPs	744.5380	459.8800	5.82	2.54	0.0000	0.0000	1.09
22	PE(18:1_18:2)	GPs	740.5141	413.3360	6.19	2.63	0.0000	0.0000	1.07
23	PE(18:2_18:2)	GPs	738.5014	373.1055	18.89	4.24	0.0000	0.0000	1.01
24	PE(36:2)	GPs	742.5301	459.9010	6.27	2.65	0.0000	0.0000	3.50
25	PE(36:4)	GPs	740.5224	371.0800	60.95	5.93	0.0000	0.0000	1.06
26	PE(38:3)	GPs	770.5518	447.1530	791.33	9.63	0.0000	0.0000	3.29
27	PE(P-18:0_18:2)	GPs	726.5350	482.2770	3.45	1.78	0.0000	0.0000	3.03
28	PE(P-18:0_22:4)	GPs	778.5678	501.3170	11.64	3.54	0.0000	0.0000	1.11
29	PG(16:0_20:2)	GPs	773.5268	375.7060	41.22	5.37	0.0000	0.0000	1.94
30	PG(37:1)	GPs	789.5724	442.1090	580.13	9.18	0.0000	0.0000	1.56
31	PG(37:2)	GPs	787.5604	430.5310	8373.60	13.03	0.0000	0.0000	1.78
32	PG(39:2)	GPs	815.5897	446.3585	165.00	7.37	0.0000	0.0000	1.30
33	PI(18:0_20:4)	GPs	885.5395	351.6230	37.19	5.22	0.0000	0.0000	2.49
34	PI(18:2_18:0)	GPs	861.5409	363.4630	51.17	5.68	0.0000	0.0000	1.89
35	PI(20:3_18:0)	GPs	887.5512	376.6240	18.54	4.21	0.0000	0.0000	1.87
36	PI(38:4)	GPs	904.5915	357.9780	154.31	7.27	0.0000	0.0000	1.35
37	PS(18:0_18:2)	GPs	786.5197	376.5580	10.08	3.33	0.0000	0.0000	3.10
38	SM(d36:1)	SPs	775.5859	431.4550	1477.60	10.53	0.0000	0.0000	1.63
39	SM(d47:1)	SPs	885.7682	686.3400	0.08	-3.67	0.0000	0.0000	2.09
40	SM(d48:1)	SPs	899.7778	679.5890	0.20	-2.35	0.0000	0.0000	1.62
41	DG(18:0_16:0_0:0)	GLs	614.5658	529.8015	0.21	-2.24	0.0000	0.0000	1.04
42	DG(18:1_16:0_0:0)	GLs	612.5572	529.8015	0.22	-2.21	0.0000	0.0000	4.05
43	DG(18:2_16:0_0:0)	GLs	610.5414	497.8680	0.09	-3.42	0.0000	0.0000	6.14
44	DG(18:2_18:0_0:0)	GLs	638.5727	533.3275	0.13	-2.93	0.0000	0.0001	3.27

45	DG(18:2_18:1_0:0)	GLs	636.5560	502.1700	0.07	-3.82	0.0001	0.0001	3.84
46	DG(18:2_18:2_0:0)	GLs	634.5394	468.6820	0.04	-4.68	0.0002	0.0002	3.16
47	DG(18:3_18:2_0:0)	GLs	632.5234	434.4805	0.01	-6.21	0.0000	0.0000	1.30
48	TG(14:0_14:0_12:0)	GLs	712.6443	640.1155	0.16	-2.64	0.0000	0.0000	1.56
49	TG(16:0_16:0_16:0)	GLs	824.7598	730.5325	0.11	-3.21	0.0001	0.0002	3.38
50	TG(16:0_14:0_12:0)	GLs	740.6746	665.2735	0.20	-2.35	0.0000	0.0000	2.12
51	TG(16:0_14:0_14:0)	GLs	768.7064	687.6620	0.31	-1.69	0.0001	0.0002	2.09
52	TG(16:1_16:1_16:1)	GLs	818.7135	670.5850	0.27	-1.88	0.0000	0.0000	6.27
53	TG(16:1_12:0_12:0)	GLs	710.6285	615.6605	0.22	-2.19	0.0000	0.0000	1.61
54	TG(16:1_14:0_12:0)	GLs	738.6598	641.9630	0.21	-2.27	0.0000	0.0000	2.59
55	TG(16:1_14:0_14:0)	GLs	766.6819	645.0450	0.13	-2.90	0.0000	0.0000	1.67
56	TG(16:1_16:1_12:0)	GLs	764.6656	622.1550	0.10	-3.37	0.0000	0.0000	1.02
57	TG(16:1_16:1_14:0)	GLs	792.6994	647.5890	0.10	-3.30	0.0000	0.0000	1.76
58	TG(16:1_16:1_16:0)	GLs	820.7301	670.6070	0.26	-1.92	0.0000	0.0000	2.22
59	TG(17:1_17:1_17:1)	GLs	860.7603	703.8460	0.28	-1.83	0.0000	0.0000	3.51
60	TG(18:1_18:1_18:1)	GLs	902.8157	737.3965	0.54	-0.89	0.0017	0.0023	4.04
61	TG(18:1_14:0_12:0)	GLs	766.6911	666.1965	0.25	-1.98	0.0000	0.0000	4.21
62	TG(18:1_14:0_14:0)	GLs	794.7147	687.9840	0.62	-0.69	0.0000	0.0000	2.85
63	TG(18:1_16:0_16:0)	GLs	850.7766	731.8000	0.75	-0.41	0.0000	0.0000	3.15
64	TG(18:1_16:1_16:1)	GLs	846.7358	673.6590	0.25	-2.00	0.0000	0.0000	2.62
65	TG(18:1_17:0_16:0)	GLs	864.7991	745.8970	0.28	-1.84	0.0000	0.0001	2.53
66	TG(18:1_18:0_17:0)	GLs	892.8208	746.8950	0.18	-2.48	0.0000	0.0000	1.68
67	TG(18:1_18:1_14:0)	GLs	848.7699	711.5900	0.92	-0.12	0.0049	0.0061	1.71
68	TG(18:1_18:1_15:0)	GLs	862.7834	723.5100	0.46	-1.12	0.0004	0.0005	2.69
69	TG(18:2_18:2_18:2)	GLs	896.7585	680.1540	0.20	-2.36	0.0000	0.0000	8.69
70	TG(18:2_12:0_12:0)	GLs	736.6439	619.3650	0.16	-2.69	0.0000	0.0000	2.57
71	TG(18:2_14:0_12:0)	GLs	764.6757	645.0535	0.14	-2.89	0.0000	0.0000	4.82
72	TG(18:2_14:0_13:0)	GLs	778.6892	656.4145	0.09	-3.54	0.0000	0.0000	1.18
73	TG(18:2_16:0_12:0)	GLs	792.7070	668.0085	0.26	-1.95	0.0000	0.0000	5.72
74	TG(18:2_16:0_14:0)	GLs	820.7378	690.3970	0.67	-0.58	0.0000	0.0000	3.94
75	TG(18:2_16:0_16:0)	GLs	848.7602	710.7360	0.95	-0.07	0.0394	0.0451	1.16
76	TG(18:2_16:1_12:0)	GLs	790.6908	647.9090	0.10	-3.38	0.0000	0.0000	5.03
77	TG(18:2_16:1_15:0)	GLs	832.7361	683.1260	0.17	-2.59	0.0001	0.0001	1.86
78	TG(18:2_16:1_16:1)	GLs	844.7277	654.6980	0.08	-3.63	0.0000	0.0000	2.22
79	TG(18:2_18:1_17:0)	GLs	888.7999	725.2380	0.23	-2.13	0.0000	0.0000	4.12
80	TG(18:2_18:1_18:0)	GLs	902.8042	745.1630	0.39	-1.37	0.0000	0.0000	6.40
81	TG(18:2_18:1_18:1)	GLs	900.7813	700.7115	0.42	-1.26	0.0000	0.0000	2.68
82	TG(18:2_18:2_12:0)	GLs	816.7061	651.2440	0.09	-3.55	0.0000	0.0000	5.38
83	TG(18:2_18:2_13:0)	GLs	830.7191	663.5045	0.07	-3.92	0.0000	0.0000	1.31
84	TG(18:2_18:2_14:0)	GLs	844.7367	674.1880	0.26	-1.96	0.0000	0.0000	6.98
85	TG(18:2_18:2_15:0)	GLs	858.7434	684.9465	0.00	-7.90	0.0066	0.0081	2.00
86	TG(18:2_18:2_16:0)	GLs	872.7587	695.7310	0.75	-0.41	0.0000	0.0000	3.85
87	TG(18:2_18:2_16:1)	GLs	870.7430	677.3020	0.00	-10.81	0.0063	0.0077	4.73
88	TG(18:2_18:2_17:0)	GLs	886.7837	705.3750	0.17	-2.59	0.0000	0.0000	3.81
89	TG(18:2_18:2_17:1)	GLs	884.7588	686.0960	0.09	-3.46	0.0000	0.0000	2.82
90	TG(18:2_18:2_18:0)	GLs	900.8006	717.3635	0.52	-0.93	0.0000	0.0000	4.87
91	TG(18:2_18:2_18:1)	GLs	898.7749	679.5970	0.19	-2.38	0.0000	0.0000	3.57

92	TG(18:3_12:0_12:0)	GLs	734.6284	594.7420	0.04	-4.74	0.0000	0.0000	1.58
93	TG(18:3_14:0_12:0)	GLs	762.6591	622.5000	0.10	-3.33	0.0000	0.0000	2.79
94	TG(18:3_16:1_12:0)	GLs	788.6739	626.4770	0.05	-4.38	0.0000	0.0000	2.74
95	TG(18:3_18:1_18:1)	GLs	898.7840	699.3520	0.34	-1.58	0.0000	0.0000	6.85
96	TG(18:3_18:2_12:0)	GLs	814.6905	631.4940	0.05	-4.23	0.0000	0.0000	2.02
97	TG(18:3_18:2_14:0)	GLs	842.7212	655.3470	0.06	-4.06	0.0000	0.0000	6.05
98	TG(18:3_18:2_15:0)	GLs	856.7352	667.0590	0.05	-4.25	0.0000	0.0000	1.59
99	TG(18:3_18:2_16:1)	GLs	868.7381	658.1890	0.07	-3.91	0.0000	0.0000	6.12
100	TG(18:3_18:2_17:1)	GLs	882.7481	669.7355	0.05	-4.30	0.0000	0.0000	1.26
101	TG(18:3_18:2_18:2)	GLs	894.7431	661.8040	0.00	-13.25	0.0061	0.0075	4.85
102	TG(18:3_18:3_14:0)	GLs	840.7064	635.8275	0.05	-4.34	0.0000	0.0000	1.79
103	TG(18:3_18:3_16:1)	GLs	866.7222	639.8910	0.02	-5.75	0.0000	0.0000	1.67
104	TG(18:3_18:3_18:2)	GLs	892.7543	642.9060	0.05	-4.43	0.0001	0.0002	3.18
105	TG(19:0_18:2_18:1)	GLs	916.8192	750.2440	0.09	-3.56	0.0000	0.0000	2.40
106	TG(19:0_18:2_18:2)	GLs	914.8140	727.0000	0.14	-2.83	0.0000	0.0000	1.48
107	TG(20:1_18:2_17:0)	GLs	916.8300	747.7640	0.09	-3.56	0.0000	0.0000	2.38
108	TG(20:4_18:2_18:2)	GLs	920.7546	653.8450	0.06	-4.08	0.0000	0.0000	1.30
109	TG(22:4_18:1_16:0)	GLs	926.8029	725.2610	0.48	-1.07	0.0000	0.0000	1.45
110	TG(22:5_18:1_16:0)	GLs	924.7989	706.8010	0.38	-1.38	0.0000	0.0000	1.74

Rt, retention time; FDR, false discovery rate; VIP, variable importance in projection; GPs, glycerophospholipids; GLs, glycerolipids.

Table S2: Receiver operating characteristic parameter.

No.	Lipid name	AUC	Ci1	Ci2	Specificity (%)	Sensitivity (%)	Threshold
1	PC(O-18:2/18:2)	1	1	1	1	1	246822.04
2	PC(O-18:2/18:1)	1	1	1	1	1	243441.83
3	PC(32:2)	1	1	1	1	1	177837.08
4	PC(O-18:2)	1	1	1	1	1	343465.10
5	PC(38:6)	1	1	1	1	1	60111.42
6	PE(38:3)	1	1	1	1	1	527351.59
7	LPE(O-18:2)	1	1	1	1	1	114465.20
8	PG(37:2)	1	1	1	1	1	343.94
9	PG(39:2)	1	1	1	1	1	106775.26
10	PI(38:4)	1	1	1	1	1	87580.11
11	SM(d36:1)	1	1	1	1	1	190095.29

Area under the receiver operating characteristic (ROC) curve (AUC) was the area under ROC curve, Ci1 is the lower limit of AUC confidence interval; Ci2 is the upper limit of AUC confidence interval.

Table S3: Data quality control of Illumina Paired-end sequencing and assembly as well as annotation on unigenes in different databases for Dezhou donkey.

Item	LDM	VAT
Raw reads	55625304±1731486	56904916±1201097
Total raw bases (bp)	8399420870±261454456	8592642249±181365688
After trimming (clean reads)		
Clean reads	55118798±1721661	56402656±1200757
Clean bases (bp)	8105538257±256289176	8303496879±180659244
Error rate(%)	0.0239±0.0001	0.0241±0.0001
Q20 (%)	98.42±0.04	98.33±0.05
Q30 (%)	95.33±0.09	95.03±0.12
GC content (%)	54.33±0.11	50.70±0.14
After de novo assembly		
Total sequence base	138936	
Total unigenes num	154948346	
Average length	1115.25	
E90N50	6342	
GC percent	47.02	
BUSCO score (%)	82.30	
Database	Annotation	Ration (%)
GO	20587	14.82
KEGG	20300	15.61
COG	24000	17.27
NR	39202	28.22
Swiss-Prot	26119	18.80
Pfam	17537	12.62
Total annotation	40696	29.29
Total	138936	100

Q20 and Q30: the sequencing error rate 0.01 and 0.001 respectively.
GO, Gene Ontology; KEGG, Kyoto Encyclopedia of Genes and Genomes; COG, Clusters of Orthologous Groups; NR, Non-Redundant Protein Sequence Database.